International Journal of Biological, Life and Agricultural Sciences
ISSN: 2415-6612
Vol:7, No:9, 2013

Cooling of Fresh Vegetable Farm Produce: Experimental and Numerical Studies

Hala Yassine, Hervé Noel, Pascal Le Bideau, and Patrick Glouannec

***Abstract*—**Following harvest, fresh produce needs to be cooled immediately in a room where the air temperature and the relative air humidity are controlled to maintain the produce quality. In this paper, an experimental study for forced air cooling of fresh produce (cauliflower) is performed using a pilot developed within our laboratory. Furthermore, a numerical simulation of spherical produces, taking into account the aerodynamic aspect and also the heat transfer in the produce and in the air, was carried out using a finite element method. At the end of this communication, experimental results are presented and compared with the simulation.

***Keywords*—**Cauliflower, Forced air cooling, Heat transfer, Numerical model, Tunnel of air.

I. Introduction

THE temperature of farm produces (fruits and vegetables) during the harvest is closed to the ambient temperature. The effective management of temperature is essential to guarantee an acceptable produce quality several days after the harvest. Rapid reduction of produces temperature to the optimum storage conditions have lead to produces with desired quality and prolonged their shelf life [1]. For fruits and vegetables, a compromise must be found between a low storage temperature (but above the freezing temperature) and a temperature that ensures the balance of biochemical reactions that are slowed. Moreover, in order to minimize weight loss in fruits and vegetables, it is important to set the store air at a value of the relative humidity (RH) as high as possible, typically 90-97% RH. However, excessive levels of RH, in certain cases, may encourage microbial spoilage and it is thus necessary to ensure that the humidity in the store remains within acceptable limits [2]. Generally, humidity is more difficult to control than temperature and often does not receive adequate consideration in the design of cold storages rooms.

This communication deals with the cooling of cauliflower. This vegetable, which is very climate-sensitive, is currently cultivated in temperate climates. As a great part of the production is exported, this produce requires a temperature conditioning before being transported.

Usually six to eight cauliflowers are placed in perforated bins before being conditioned. The optimal storage conditions for the commercialization of this fresh produce are between 4°C-7°C and between 85-95% [3].

Hala Yassine is with the Univ Bretagne Sud, LIMATB, EA 4250, Rue de St Maude, F-56100, Lorient, France (corresponding author; phone: 33-297874517; e-mail: hala.yassine@ univ-ubs.fr).

This produce has been the subject of little investigation [4] but we can identify several studies which have dealt with the conditioning of fresh foodstuffs.

Experimental aerodynamic and thermal studies have been carried out by Alvarez and Flick [1], [5] to obtain a better understanding of the forced convection cooling of spheres placed in bins. The authors observed the heterogeneous evolution of temperatures during cooling.

Other authors [6]-[10] used a zonal model to study the processes of heat and mass transfer in bins filled with apples.

Alvarez and Flick [11] used a macro-porous media approach to predict cooling kinetics of stacked produces.

Nachor et al. [12] used a computational fluid dynamics (CFD) modeling to predict airflow distribution, produce temperature, and produce weight loss in cold-stored pears. Dehghannya, Nagdi, and Vigneault [13], [14] carried out aerodynamic and thermal analysis for the forced convection cooling of the spheres stacked in three different packages opening configurations. More uniform air flow distribution can be obtained by increasing the vent area from 2.4 to 12.1%. Ferrua and Singh [15], [16] modeled the forced-air cooling process of fresh strawberries in 3D. The results showed that the heterogeneity of the cooling process is largely influenced by the structure and design of the packaging system.

Gowda, Narasimham, and Nurthy [17] have developed a non-dimensional mathematical model for forced-air pre-cooling of spherical foods in bulk. They have defined the best operating parameters for pre-cooling systems. Martins, Olivier, and Saraz [18] studied the change in temperature around two apples in tandem arrangement in a air tunnel at different Reynolds numbers and then assessed the Nusselt number around these two apples.

The aim of this communication is to study the experimental and modeling aspects of the cooling of fresh produces (cauliflower).

II. Description of Experience

The cooling experiments are carried out using a pilot developed within our laboratory. It consists of a large ventilation duct with a rectangular cross-section coupled with an air loop. The ventilation duct has the following dimension: length of 2m, width of 0.385m and height of 0.31m. The origin of the Cartesian coordinate system is the center of the tunnel at a distance of 0.3m from the inlet. In this air duct, a produce with an average diameter about 16cm is placed at 1.1m from the Cartesian coordinate's origin (see Figs. 1 and

2). The air temperature and the air humidity at the inlet are imposed by means of an air handling unit.

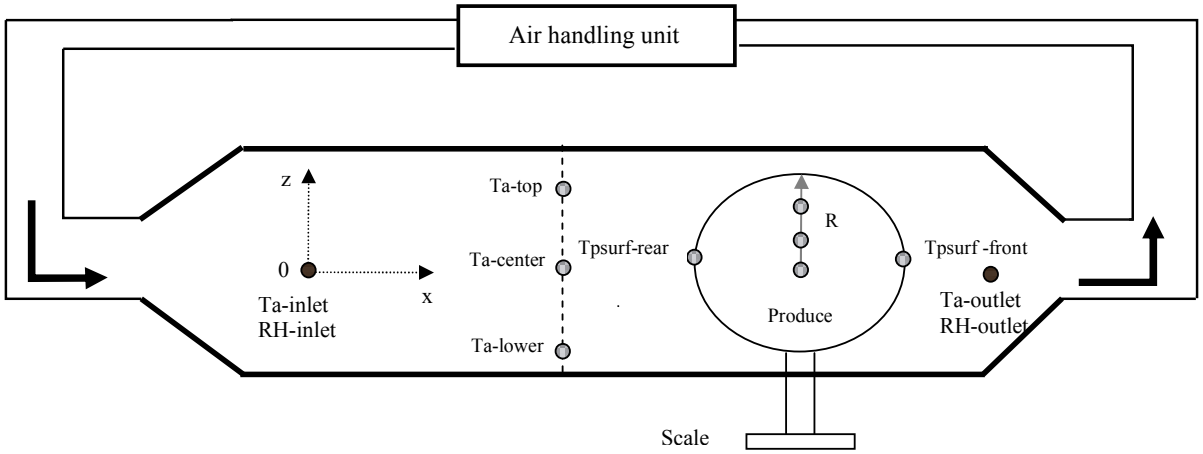

Fig. 1 Schematic diagram of the cooling pilot (side view)

The bottom and side walls are constituted of a Styrofoam-type insulating. A removable Plexiglas window has been arranged on the upper surface of the tunnel to handle the produce and to monitor the experiment.

A. Instrumentation of the Tunnel of Air

The objective is to establish temperature and velocity profiles to confirm the model that will be developed (see Figs. 1 and 2).

A continuous measurement of the inlet and outlet aero-thermal conditions is performed: the air velocity is taken with an anemometer whereas wet and dry air temperatures are measured with a psychrometer. These last measurements allow the calculation of the relative humidity.

K-type thermocouples are also positioned before the produce to measure air temperature in the tunnel at different widths and heights. Moreover, independent measures of air velocity have been carried out at different points in the tunnel of air with and without produce.

B. Instrumentation of the Produce

The produce temperature is measured at several positions with K-type thermocouples. A stainless steel sheathed thermocouple is placed in the center of the produce and two others at a distance of R/3 and 2R/3 from the center (Fig. 1). In addition, the surface temperature of the produce is measured at three positions (front-rear-lateral) with micro thermocouples. The mass of the produce is continuously measured using a 0.1g precision scale disposed under the cooling tunnel.

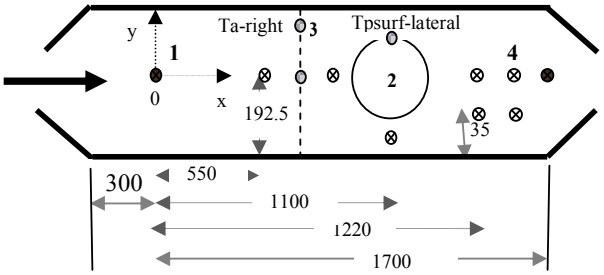

Fig. 2 Schematic of the air tunnel and the positions of thermocouples in the tunnel (top view) 1-Psychrometers, 2- Produce, 3- K-Thermocouples, 4- Holes to put thermocouples and anemometers

III. Numerical Model

The objective is to simulate the velocity and the temperature fields in the tunnel of air and in the produce. Model without produce and other with produce are developed.

The air inside the tunnel is considered as an incompressible fluid with constant properties. The mass transfer in the produce and in the air is neglected.

The velocity at the inlet of the tunnel is between 0.8 m/s and 1 m/s, what respectively corresponds to Reynolds number of 19625 and 24532 in the tunnel.

A. Model Formulation

The governing mass, momentum and energy conservation equations for the air domain are written [13], [19]:

$$\rho_a \nabla.(u) = 0 \quad (1)$$

$$\rho_a (u.\nabla)u = \nabla.[pI + \tau] \quad (2)$$

$$\rho_a C_{p,a} \frac{\partial T_a}{\partial t} + \rho_a C_{P,a} u.\nabla T_a = \nabla.(k_a \nabla T_a) \quad (3)$$

With the viscous stress tensor τ in Pa:

$$\tau = \mu_a(\nabla u + (\nabla u)^T) - \frac{2}{3}\mu_a(\nabla . u)I. \quad (4)$$

and the aero-thermal conditions : u air velocity m/s, p pressure Pa, T_a air temperature K, the thermo-physical properties: ρ_a the air density kg/m^3, μ_a air dynamic viscosity kg/(m.s), $C_{p,a}$ air specific heat capacity J/(kg.K), k_a air thermal conductivity W/(m.K)

The boundaries conditions can be written as:

- On the inlet of the tunnel (x=0):

$$u = u_0,\ T_a = T_0$$

- On the outlet of the tunnel (x=L):

$$\left[\mu(\nabla u + (\nabla u)^T) - \frac{2}{3}\mu(\nabla . u)I\right] = 0, p = p_0 = 0, (-k_a \nabla T_a) = 0$$

- On all wall of the tunnel:

$$u = 0\ , (-k_a \nabla T_a) = h_{cp}(\ T_{amb} - T_{pa})$$

- On planes of symmetry:

$$u = 0, (-k_a \nabla T_a) = 0$$

with $h_{cp}$the heat transfer coefficient between the walls of the tunnel and the exterior W/(m^2.K), T_{pa} walls temperature and it is taken equal to the exterior air temperature.

For the produce, the energy conservation equation neglecting the heat of respiration (usually small compared to the effects of sensible heat) is written [19]:

$$\rho_p c_{p,p} \frac{\partial T_p}{\partial t} = \nabla\left(k_p \nabla T_p\right) \quad (5)$$

with the thermal conditions: T_p produce temperature K and the thermo-physical properties: ρ_p produce density kg/m^3, $c_{p,p}$ produce specific heat capacity J/(kg.K), k_p produce thermal conductivity W/(m.K).

The initial conditions:

$$T_p(r, t = 0) = T_{p0} = const$$

The boundary conditions:

- On the produce surface: $T_p(r = R, t) = T_a$

B. Numerical Method

COMSOL Multiphysics software is used to solve the air flow and heat transfer models for this 3D problem. Once the momentum balance is computed and the velocity field is known, the conservation of energy is solved as a time dependent process.

The produce is considered as a sphere of diameter 16 cm. A quarter of the tunnel with two symmetries is modeled as shown in Fig. 3. A normal mesh with approximately 188000 elements is used. The finite element computation of incompressible flows involves numerical instabilities. To avoid these instabilities streamline diffusion and crosswind diffusion conditions were used.

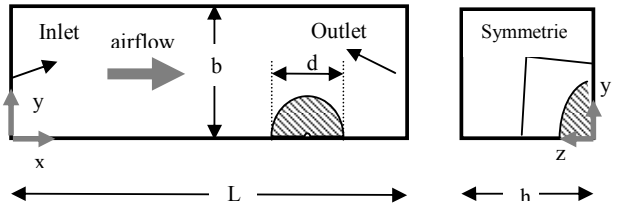

Fig. 3 Computational domain for the tunnel with sphere model (1/4 sphere, left: side view, right: frontal view)

IV. Results and Discussion

A. Study of the Air Tunnel

The air velocity profile is measured at different positions in the tunnel in two different cases: once when the tunnel is empty (without produce) and again when there is a foam ball inside the tunnel. Furthermore, other experimental tests are performed for the tunnel with cauliflower to study the evolution of the air temperature and its relative humidity in the tunnel and to measure the evolution of the cauliflower temperature at different positions.

1. Experimental and Numerical Aerodynamic Study

a) Without Produce

Presentation of Experimental Results

Experimental measurements without produce are carried out to find the profile of the air velocity in different positions in the tunnel.

The air velocity at different positions x with the height z is shown in Fig. 4.

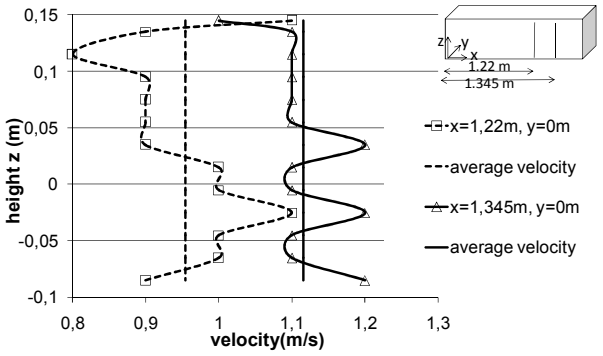

Fig. 4 Evolution of the velocity at different positions x in the tunnel with the height z (without produce)

The evolution of the air velocity at the same length x and at different width y gives in Fig. 5.

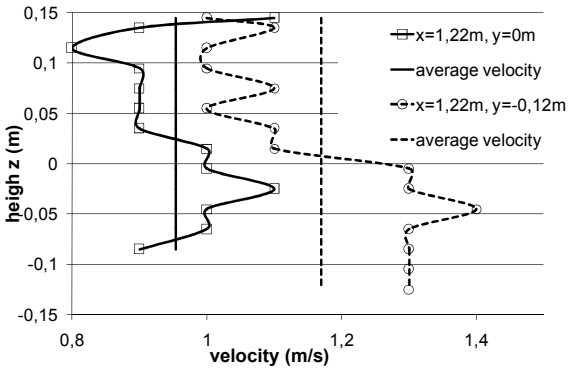

Fig. 5 Evolution of the velocity at different positions y in the tunnel with the height z (without produce)

Based on Fig. 5, we note that the air velocity at distance 1.22m from the inlet of the tunnel (the Cartesian coordinate's origin) is quasi-uniform between the height (0.1 ÷ -0.1) m, with value 1.20 ± 0.2 m/s. This position corresponds to the section where the produce will be placed. We note that the closer to the tunnel outlet, the air flow is more homogeneous. The perturbations in the air velocity visible at the inlet can be related to the effect of the geometry of air duct which connects the air handling unit with the tunnel.

Simulation –Experimental Comparison

Simulation test for the empty tunnel is performed using COMSOL software to compare the velocity profiles numerically obtained with experimental ones. This simulation test is achieved under the same conditions of the experimental: the air is blown at the inlet at constant velocity 1 m/s along the height *z*. Fig. 6 presents a comparison between the average values of the velocity experimentally measured with the simulated velocity profiles. In this simulation, we present the comparison on the half of the height *z* of the tunnel because the velocity has symmetry profile relative to the middle of the tunnel as we have seen in the experimental results.

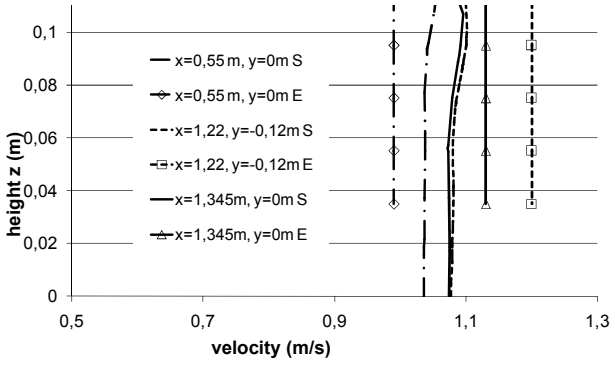

Fig. 6 Comparison of the velocity of the air at different positions x, y in the tunnel, (S)-Simulation, (E)-Experimental (without produce)

In this comparison, we are particularly interested in the velocity at the produce level which it does not exceed the height of 0.11m. We note that the experimental and simulated velocities are closed to each other; their difference could be explained by experimental errors. Therefore, the model is satisfied for the height between 0m and 0.11m.

b) With Foam Ball

Presentation of Experimental Results

A cooling experimental test is performed with foam ball of diameter 16-17cm, which is the same diameter of a cauliflower.

In this section, we present the air velocity measures carried out before and after the foam ball. These measurements at different positions x, y in the tunnel with the height *z* is given in Figs. 7 and 8.

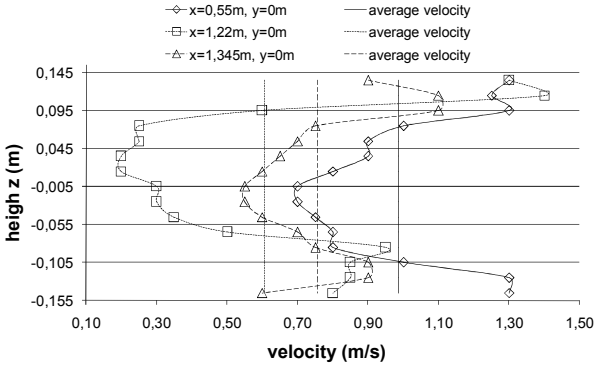

Fig. 7 Evolution of the velocity for y=0 at different positions x and z in the tunnel (with foam ball)

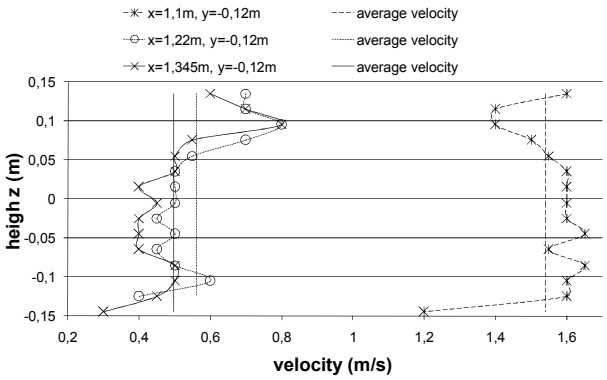

Fig. 8 Evolution of the velocity for y=0.12 m at different positions x and z in the tunnel (with foam ball)

In the section where the produce is present (at x = 1.1m) the air velocities are larger and have almost constant value along the height *z* (Fig. 8). This increase in velocity is due to the decrease of the passage section. Just behind the foam ball (Figs. 7 and 8); the air velocities strongly decrease while larger values are measured close to the walls.

Simulation-Experimental Comparison

A comparison between the average values of the velocity experimentally measured with the simulated velocity profiles before the foam ball is shown in Fig. 9. A good agreement

between the results of the experiments and the simulations is obtained.

Fig. 10 presents a comparison between the simulation and the experimental of the air velocity profile behind the produce at different positions x and at the same width y=0 (middle of tunnel), respectively. We notice that the velocity curves obtained by the simulation do not have exactly the same values as that obtained by the experimental, but they have the same aspect. This may be related to uncertainty of the measure.

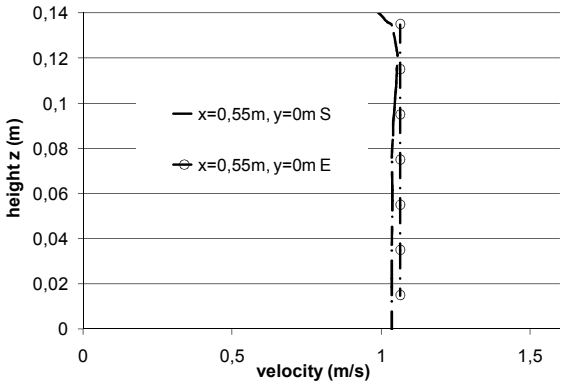

Fig. 9 Comparison of the velocity at different positions x in the tunnel before the produce, (S)-Simulation, (E)-Experimental (with foam ball)

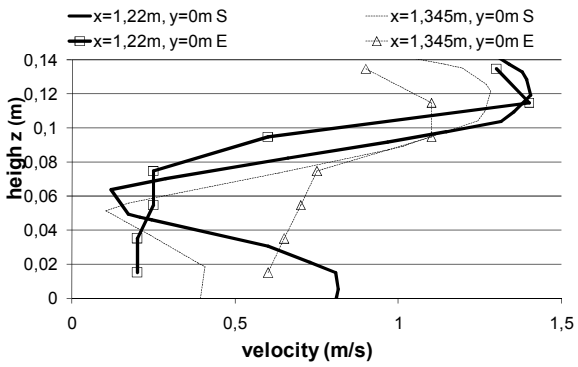

Fig. 10 Comparison of the velocity at different positions x in the tunnel after the produce, (S)-Simulation, (E)-Experimental (with foam ball)

2. Experimental and Numerical Thermal Study

To study the evolution of the air temperature and the air humidity at both the inlet and the outlet of the tunnel, a 16 cm diameter cauliflower was cooled for six and a half hours in the tunnel. This cauliflower is placed in the tunnel when the temperature and the relative humidity of the air has reached the set-point and got stabilized. The air temperature is kept constant at about 2.1°C and the relative humidity of the air is around 82.4%. The average velocity of the air in this experimental is 0.89 m/s and the air mass-flow is 0.13 kg/s. The initial temperature of the cauliflower is 11.5°C at the center and 6.5°C at the surface. The initial mass is 918.67 g.

The temperature at different positions in the tunnel in the *yz* section is measured by using thermocouples positioned upstream of the produce. The evolution of these temperatures with the cooling time is shown in Fig. 11, and the comparison of these temperatures with the simulation is presented in Fig. 12. We notice that the temperature in these positions have the same value, so we can consider that the temperature in the *yz* section of the tunnel is homogeneous (Fig. 11). The comparison shows an acceptable agreement between the simulated and experimental air temperatures upstream of the produce (Fig. 12), the difference in the values of temperature between the experiment and the simulation can be related to uncertainty of the measure: the difference in the accuracy of the sensors used to measure the temperature at the inlet (Psychrometer), and the ones used to measure the temperature ahead the produce (K-type thermocouples).

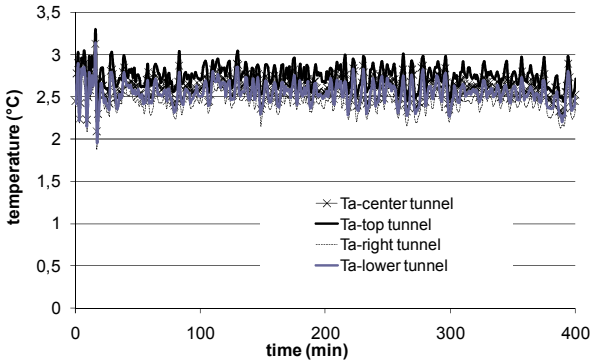

Fig. 11 Evolution of the air temperature at different positions in the yz section in the tunnel (with produce)

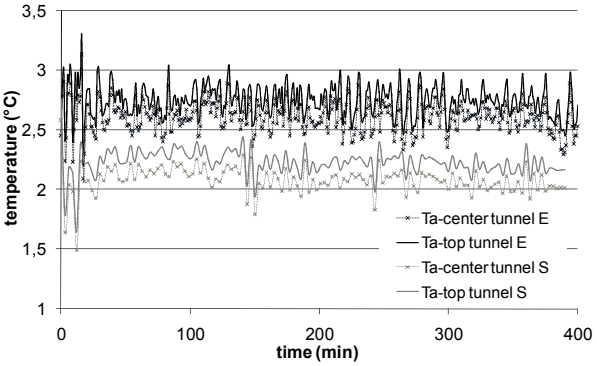

Fig. 12 Comparison of the temperature of the air before the produce, (S)-Simulation, (E)-Experimental (with produce)

The evolution of the relative humidity and the temperature of the air at the inlet and the outlet of the tunnel are shown in Figs. 13 and 14, respectively.

It can be noticed that the relative humidity at the outlet is greater than that at the inlet; this increase is related to the evaporation of water at the produce surface.

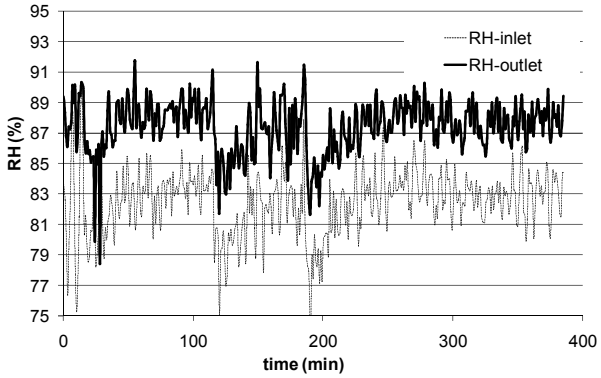

Fig. 13 Evolution of the relative humidity of the air at the inlet and the outlet of the tunnel (with produce)

The air temperature increases at the outlet of the tunnel. This increase is related on one side to the heat which has been derived from the produce during the passage of air above it, and on the other side to the heat gain through the walls of the tunnel.

A comparison between the experiment and the simulation for the evolution of the air temperature at the inlet and at the outlet of the tunnel is presented in Fig. 13. We note that there is acceptable agreement between simulated and experimental air temperatures at the inlet and outlet of the tunnel.

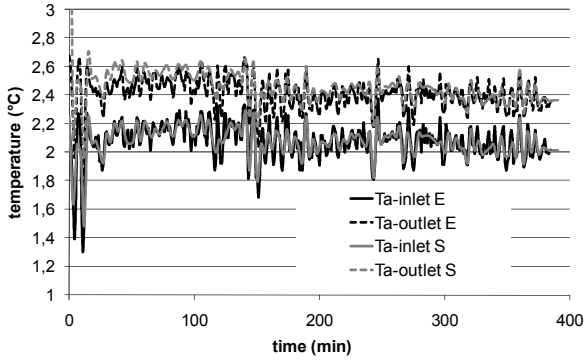

Fig. 14 Comparison of the air temperature at the inlet and the outlet of the tunnel, (S)-simulation, (E)-Experimental (with produce)

B. Study of the Produce

Presentation of Experimental Results

The change in the temperature of cauliflower at different positions inside the produce and at its surface is measured during the cooling process and presented in Fig. 15. It can be seen that the produce temperature decreases with the cooling time and stabilizes at a temperature close to the air temperature. We notice that the surface temperature of produce decreases faster than the temperature in the center and reaches a lower temperature. The temperature at the surface in the front position decreases faster than the other two positions (rear and side). The temperatures in the center, and in position R/3 and 2R/3 stabilize at temperature far from this of the air and these of the surface, this can be explained by the accuracy of the thermocouples used, car the thermocouples used to measure the surface temperature are not the same kind of these used to measure the temperature in the center, and in position R/3 and 2R/3.

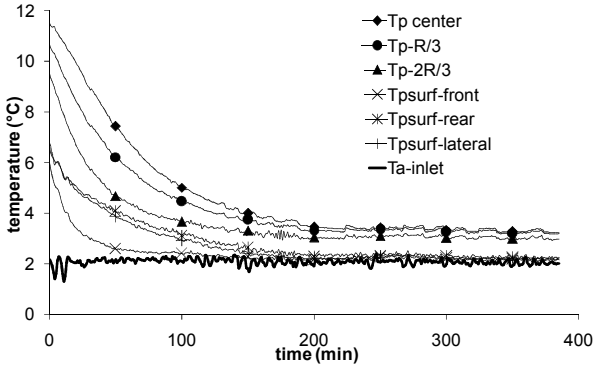

Fig. 15 Evolution of the produce temperature at different positions in the produce and at the surface

Fig. 16 presents the evolution of the mass of the cauliflower with cooling time. The mass of the produce decreases over time. At the end of the cooling, the net mass of the cauliflower is 903 g. This decrease is due to evaporation of water at the surface of the produce.

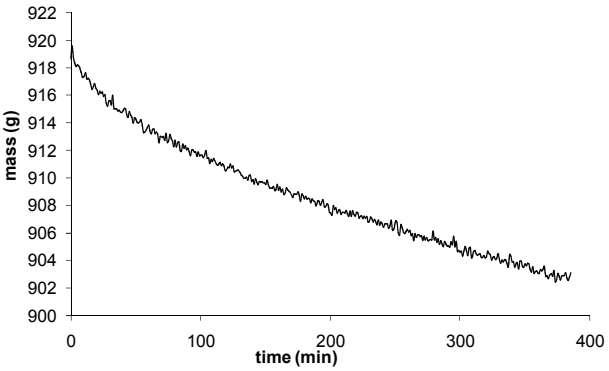

Fig. 16 Evolution of the mass of the produce with the cooling time

Simulation-Experimental Comparison

Fig. 17 presents the simulation-experimental comparison for the change in the produce surface temperature at different positions. We notice that the produce surface temperature in the front position decreases faster than in the lateral and rear positions in both cases (experimental and simulation) and they have similar values. As regards the evolution of the produce surface temperature in the lateral and rear position we see that there is grand difference between the two values in the simulation which we do not find in the experimental. Indeed, we can note that, in the simulation, the temperature value in the rear position is close to the temperature in the experiment whereas the simulated and experimental temperatures in the lateral position do not have the same value.

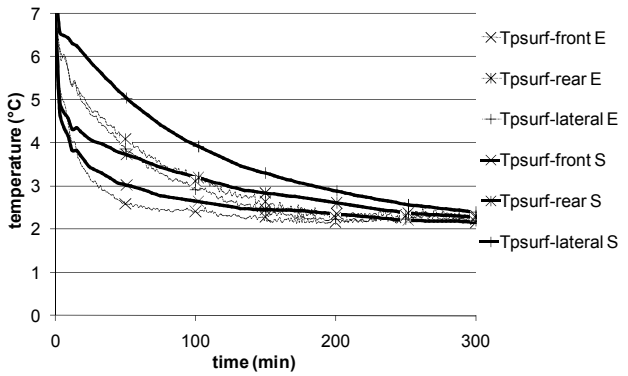

Fig. 17 Comparison of the evolution of the produce surface temperature at different positions, (S)-Simulation, (E)-Experimental

Fig. 18 shows the simulation-experiment comparison of temperatures at different positions in the produce. One can notice that temperatures at the produce centre are close during the first 200 minutes. After that period, the simulated temperature decreases faster and finally reaches the value of the air temperature. Cauliflower experimental and simulated temperatures at distance R/3 and 2R/3 from the centre are rather different; the experimental temperatures decrease faster. These differences can be explained by the mass transfer in the produce which has not been taken into account and also by the use of stainless steel sheathed thermocouples which give the difference in the temperature at the end of the cooling. Enhancement in the results will be achieved by replacing these thermocouples with micro-thermocouples. Yet, some other leads are to be studied; the calculation of the exchange coefficients as well as the thermo-physical properties of these non-homogeneous produce have to be refined.

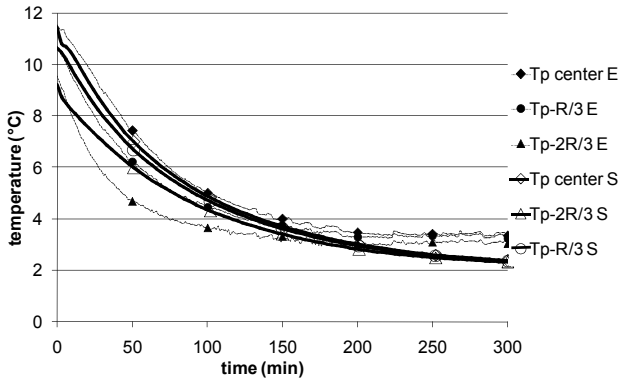

Fig. 18 Comparison of the evolution of the temperature at different positions inside the produce, (S)-Simulation, (E)-Experimental

C. Sensitivity Study

Based on the numerical simulation, the effects of deviations in the airflow velocity and in the properties of cauliflower on its cooling are studied. The reference case (ref) is carried out in the following conditions: the air temperature is kept constant about 3.7°C and the average air velocity at the inlet is 0.75m/s. the initial temperature of the cauliflower is 14.5°C at the center and 15.7°C at the surface.

TABLE I
MODEL PARAMETER AND ITS VARIATION UNDER SENSITIVITY STUDY

Properties	Model parameters	Variation
u m/s	0.75	±0.25 m/s
$C_{p,p}$ J/(kg.K)	3171	±25%
k_P W/(m.K)	0.48	±25%
ρ_p kg/m3	438	±25%

The effects of deviations in these parameters on the temperatures at the centre and on the front surface will be presented. These two temperatures are selected because they give larger gradient in the thickness of the produce.

1. Air Velocity

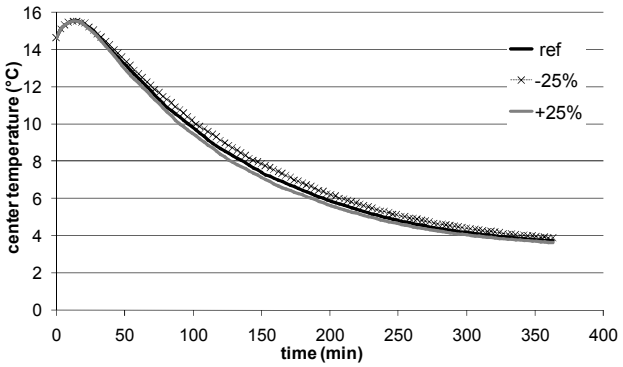

(a)

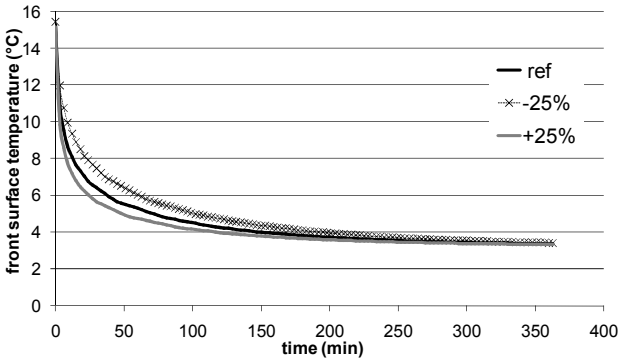

(b)

Fig. 19 Sensitivity of produce temperature to velocity inlet air, (a) center temperature, (b) front surface temperature

Fig. 19 shows the sensitivity of the centre and the front surface temperatures to the velocity of the inlet air. As expected, cooling is more effective with higher air speed. It can also be noticed that a loss in air speed has more impact than a gain in air speed.

2. Produce Properties

Heat Capacity

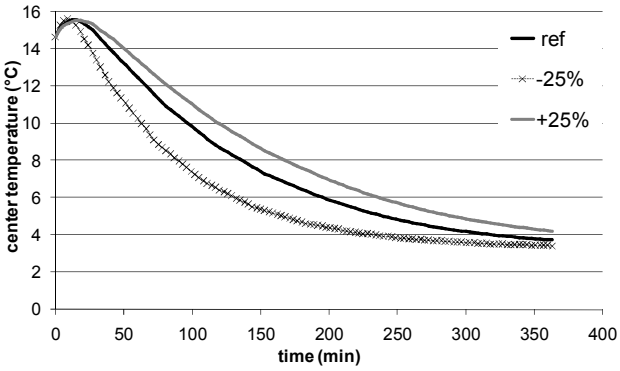

(a)

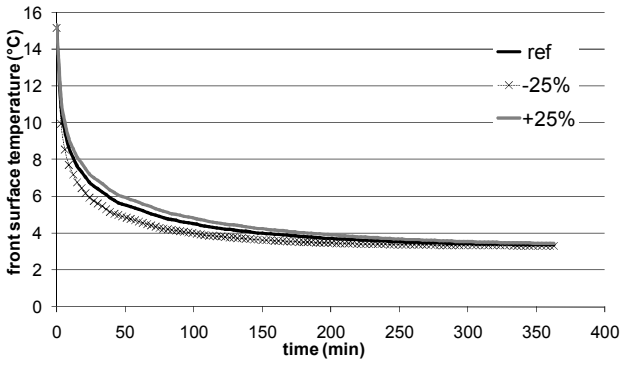

(b)

Fig. 20 Sensitivity of produce temperature to produce heat capacity, (a) center temperature, (b) front surface temperature

Fig. 20 shows the sensitivity of the centre temperature and of the front surface temperature regarding the heat capacity of the produce. The influence of the produce heat capacity on the centre temperature is more obvious than its influence on the front surface temperature. But in both cases, it is confirmed that the lower the heat capacity, the faster the cooling is.

Thermal Conductivity

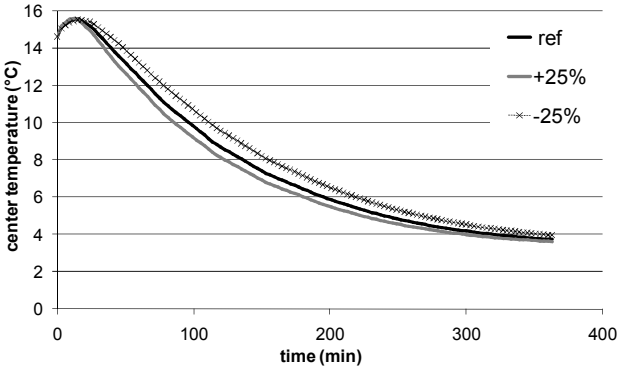

(a)

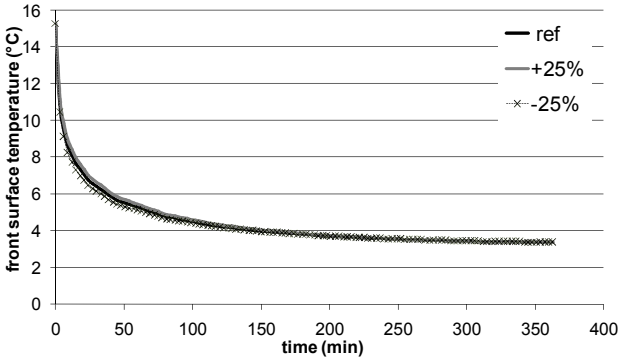

(b)

Fig. 21 Sensitivity of produce temperature to produce thermal conductivity, (a) center temperature, (b) front surface temperature

Fig. 21 shows the sensitivity of the centre temperature and the surface temperature to the thermal conductivity. In Fig. 21 (b), one can see that the front surface produce temperatures are not very sensitive to the produce thermal conductivity; however, the center temperature is more sensitive to variation of the produce thermal conductivity. A rise in the produce thermal conductivity speeds up the cooling at the produce centre.

Density

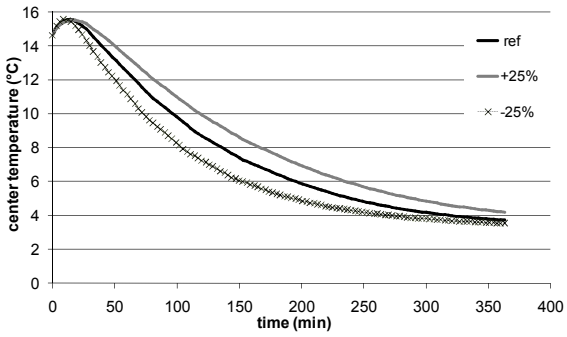

(a)

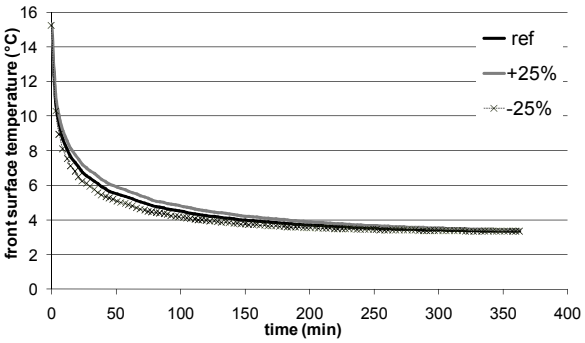

(b)

Fig. 22 Sensitivity of produce temperature to produce density, (a) center temperature, (b) front surface temperature

Figs. 22 (a) and (b) shows the centre and front surface temperatures sensitivity to the density produce. The influence of the produce density on the centre produce temperature is clear, whereas the front surface temperature is not much affected by the change in density.

D. Convective Heat Transfer Coefficient (h_c)

In this section, first we present a calculation of heat transfer coefficient from the Nusselt number and from the simulation. Next, a comparison between these two values is presented.

In the literature, several relations have been established to calculate the Nusselt numbers around a sphere in the case of laminar and turbulent flows [20], [5]. The more used correlation is due to Whitaker [18]-[20], [21]:

$$Nu = 2 + (0.4Re^{\frac{1}{2}} + 0.06Re^{\frac{2}{3}})Pr^{0.4}\left(\frac{\mu_a}{\mu_w}\right)^{1/4} \quad (6)$$

$$0.71 \leq Pr \leq 380$$
$$3.5 \leq Re \leq 7.6 * 10^4$$
$$1 \leq \frac{\mu_a}{\mu_w} \leq 3.3$$

with

Re Reynolds number: $Re = \frac{\rho_a \mathrm{u} D}{\mu_a}$

Pr Prandtl number: $Pr = \frac{\mu_a C_{p,a}}{k_a}$

The thermo-physical properties are calculated according to the mean measured air temperature.

$\rho_a = \frac{353}{T_a}$ kg/m^3

$\mu_a = 10^{-5}(0.0046(T_a - 273.15) + 1.7176)$ kg/(m.s)

$k_a = (7.57 * 10^{-5}(T_a - 273.15)) + 0.0242$ W/(m.K)

μ_w the air viscosity at produce surface

In our case: $\frac{\mu_a}{\mu_w} = 0.998 \approx 1$

And the heat transfer coefficient is given as follows:

$$h_c = \frac{Nuk_a}{D} \quad (7)$$

with D: the produce diameter m.

The heat transfer coefficient has been calculated in the simulation by dividing the heat flux at the surface of the produce by the difference in temperatures between the produce surface and the air as following:

$$h_c = \frac{\emptyset_{psurf}}{(T_{psurf} - T_a)} \quad (8)$$

with $\emptyset_{surf}$ the heat flux at the produce surface W/m^2, T_{psurf} the mean surface produce temperature K, T_a air temperature K.

Fig. 23 shows the evolution of h_c as a function of cooling time as calculated in (8).

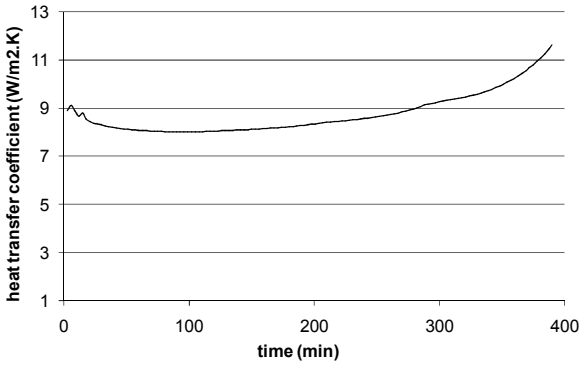

Fig. 23 Evolution of heat transfer coefficient between the produce and the air according to the simulation

A comparison of the heat transfer coefficient calculated by the Nusselt number and the average value calculated from the simulation at the same velocity of 1.2 m/s (the velocity in the section of the tunnel where the produce is located) is presented in Table II.

TABLE II
COMPARISON THE VALUE OF HEAT TRANSFER COEFFICIENT

	Value of h_c (W/m2.K)
According to the Nusselt number	11.4
According to the simulation	8.8

The difference between these two values may be explained by the effect of the tunnel walls on the flow in the simulation, because Whitaker's correlation calculates h_c around a sphere in free-flowing air (not limited by the walls).

V. CONCLUSION

This paper has presented experimental aerodynamic and thermal results for the forced-air cooling of the fresh produce placed in an air tunnel. Measures of velocities and temperatures have been compared to numerical simulations. The results have showed the necessity to improve the temperatures measurement and to take into account the water transfers in the produce. The infrared radiative heat transfer between the surfaces of wall and the produce must also be studied.

Soon, new cooling experiments of cauliflower will be achieved to obtain new results with an adequate instrumentation. In the same time, a characterization phase should be carried out to correctly apprehend the thermo-physical properties of cauliflower. Furthermore, experiments for the tunnel will be performed by using two cauliflowers (one after the other) to study the cooling kinetics in this case. Along the same lines, the numerical model should be developed for these conditions to simulate this case.

REFERENCES

[1] G. Alvarez et D. Flick, « Analysis of heterogeneous cooling of agricultural products inside bins Part I: aerodynamic study », *J. Food Eng.*, vol. 39, n° 3, p. 227 - 237, 1999.

[2] S. A. Tassou et W. Xiang, « Modelling the environment within a wet air-cooled vegetable store », *J. Food Eng.*, vol. 38, nº 2, p. 169 - 187, 1998.
[3] « Refrigeration requirements for fruits & vegetables ». Britsh Columbia Ministry of Agriculture and Food, 1989.
[4] F.Billiard, J.L. Peden, « Le froid humide application à la refrigération de chou », *Journée Française Froid*, p. 169-173, 1988.
[5] G. Alvarez et D. Flick, « Analysis of heterogeneous cooling of agricultural products inside bins: Part II: thermal study », *J. Food Eng.*, vol. 39, nº 3, p. 239 - 245, 1999.
[6] N. D. Amos, « Mathematical modeling of heat and water vapor transport in apple coolstores », Massey University, 1995.
[7] D. J. Tanner, « Mathematical modeling for design of horticultural packaging », Massey University, 1998.
[8] D.J. Tanner, A.C. Cleland, L.U. Opara, et T.R. Robertson, « A generalised mathematical modelling methodology for design of horticultural food packages exposed to refrigerated conditions: part 1, formulation », *Int. J. Refrig.*, vol. 25, nº 1, p. 33 - 42, 2002.
[9] D.J. Tanner, A.C. Cleland, et L.U. Opara, « A generalised mathematical modelling methodology for the design of horticultural food packages exposed to refrigerated conditions Part 2. heat transfer modelling and testing », *Int. J. Refrig.*, vol. 25, nº 1, p. 43 - 53, 2002.
[10] D.J. Tanner, A.C. Cleland, et T.R. Robertson, « A generalised mathematical modelling methodology for design of horticultural food packages exposed to refrigerated conditions: Part 3, mass transfer modelling and testing », *Int. J. Refrig.*, vol. 25, nº 1, p. 54 - 65, 2002.
[11] G. Alvarez et D. Flick, « Modelling turbulent flow and heat transfer using macro-porous media approach used to predict cooling kinetics of stack of food products », *J. Food Eng.*, vol. 80, nº 2, p. 391 - 401, 2007.
[12] H. B. Nahor, M. L. Hoang, P. Verboven, M. Baelmans, et B. M. Nicolaï, « CFD model of the airflow, heat and mass transfer in cool stores », *Int. J. Refrig.*, vol. 28, nº 3, p. 368 - 380, 2005.
[13] J. Dehghannya, M.l Ngadi, C. Vigneault, « Simultaneous aerodynamic and thermal analysis during cooling of stacked spheres inside ventilated packages », *Chem. Engeneering Thechnologie*, vol. 31, p. 1651-1659, 2008.
[14] J. Dehghannya, M. Ngadi, et C. Vigneault, « Mathematical modeling of airflow and heat transfer during forced convection cooling of produce considering various package vent areas », *Food Control*, vol. 22, nº 8, p. 1393 - 1399, 2011.
[15] M. J. Ferrua et R. P. Singh, « Modeling the forced-air cooling process of fresh strawberry packages, Part I: Numerical model », *Int. J. Refrig.*, vol. 32, nº 2, p. 335 - 348, 2009.
[16] M. J. Ferrua et R. P. Singh, « Modeling the forced-air cooling process of fresh strawberry packages, Part II: Experimental validation of the flow model », *Int. J. Refrig.*, vol. 32, nº 2, p. 349 - 358, 2009.
[17] B. S. Gowda, G. S. V. L. Narasimham, et M. V. K. Murthy, « Forced-air precooling of spherical foods in bulk: A parametric study », *Int. J. Heat Fluid Flow*, vol. 18, nº 6, p. 613 - 624, 1997.
[18] M. A. Martins, L. S.Oliveria, J. A. O. Saraz, « Numerical study of apple cooling in tandem arrangement », p. 158-165, 2011.
[19] S. H. Ho, L. Rosario, et M. M. Rahman, « Numerical simulation of temperature and velocity in a refrigerated warehouse », *Int. J. Refrig.*, vol. 33, nº 5, p. 1015 - 1025, 2010.
[20] A. G. Dixon, M. E. Taskin, M. Nijemeisland, E. Hugh Stitt, « Systematic mesh development for 3D CFD simulation of fixed beds: Single sphere study », *Comput. Chem. Eng.*, vol. 35, p. 1171-1185, 2011.
[21] F.P.Incropera, D.P.Dewitt, T.L.Bergman, A.S.Lavine, *Fundamentals of heat and mass transfer*. 2005.